

Decay times of excitons in latticematched InGaAs/InP single quantum wells

I. Brener, D. Gershoni, D. Ritter, M. B. Panish, and R. A. Hamm

Citation: *Applied Physics Letters* **58**, 965 (1991); doi: 10.1063/1.104457

View online: <http://dx.doi.org/10.1063/1.104457>

View Table of Contents: <http://scitation.aip.org/content/aip/journal/apl/58/9?ver=pdfcov>

Published by the [AIP Publishing](#)



Re-register for Table of Content Alerts

Create a profile.



Sign up today!



Decay times of excitons in lattice-matched InGaAs/InP single quantum wells

I. Brener,^{a)} D. Gershoni, D. Ritter, M. B. Panish, and R. A. Hamm
AT&T Bell Laboratories, Murray Hill, New Jersey 07974

(Received 29 October 1990; accepted for publication 27 December 1990)

A study of the photoluminescence decay times in lattice-matched InGaAs/InP single quantum wells grown by two different epitaxial techniques is presented. We show that these decay times can be measured directly using a nonlinear photoluminescence autocorrelation technique. A model based on the saturation of localized exciton states describes the temporal behavior and the optical nonlinearities observed very well.

The dynamical processes of carriers in bulk and layered semiconductors have been extensively studied both experimentally¹⁻⁴ and theoretically⁵ over the past few years. Time-resolved optical spectroscopy has evolved as the main tool for these experimental studies, mainly due to recent advances in short laser pulse generation. In particular, the recently developed up-conversion technique allows for a temporal resolution limited only by the exciting laser pulse width.⁴ Most of the studies have been with AlGaAs/GaAs heterostructures in which carriers recombine radiatively within the binary GaAs quantum well (QW).¹⁻⁴ A few studies have been made of the InP/InGaAs system, in which the recombination takes place within the ternary QW.^{6,7} In this letter we show that the inherent optical nonlinearities of the InP/InGaAs system can be used to measure the characteristic photoluminescence (PL) decay times in QWs. The technique consists of temporally autocorrelating the PL from the sample^{8,9} using the nonlinearity of the PL (NLPL) itself. This is much easier to implement than the up-conversion technique, and yields the same temporal resolution, limited only by the laser pulse width. We demonstrate that the temporal decay observed with this technique directly corresponds to the temporal decay of the PL intensity. The origin of the nonlinearities in the excitonic radiative recombination at low temperatures is attributed to the saturation of the density of localized exciton states. A simple rate equation model based on this assumption is in very good agreement with the experimental results. It describes the temporal behavior of the linear and nonlinear PL, and correctly predicts the relative intensities of the two.

Two samples were studied, each containing four single In_{0.53}Ga_{0.47}As/InP QWs. Sample A was grown using hydride source molecular beam epitaxy (HSMBE).¹⁰ It contained 9, 15, 30, and 47 Å QWs separated by 300 Å InP barriers. The QWs were grown on a 0.3-μm-thick InP buffer layer which was followed by 1000-Å-thick layer of lattice-matched InGaAs. Sample B was grown by metalorganic molecular beam epitaxy (MOMBE) with metalorganic group V sources.¹¹ Sample B contained 12, 23, 34, 52, and 1000 Å layers of InGaAs separated by 300 Å barriers of InP. The dimensions were determined to within 3 Å, using transmission electron microscopy (TEM). The

samples were cooled to 10 K in a He-flow cryostat, and were optically excited using tunable laser pulses of less than 0.5 ps duration. The pulses were generated at an 82 MHz repetition rate by synchronously pumping a dye laser with the compressed and frequency-doubled output of a mode-locked cw Nd:YAG laser. Rhodamine 6 G was used for excitation with energies above the InP barrier band gap and Styryl 9 was used for resonantly exciting into the InGaAs wells. The experimental setups for the optical measurements of the PL decay times and the NLPL are schematically depicted in Figs. 1(a) and 1(b), respectively.

Figures 2(a) and 2(b) show the low-temperature PL (upper curves) and NLPL (lower curves) spectra of the two samples used in this work. The NLPL spectra were obtained at zero relative delay, and they are shown for two different excitation intensities for each of the samples. A positive (negative) signal in the NLPL spectra corresponds to a super (sub) linear dependence of the PL on the excitation intensity. At a low incident laser intensity (< 10 W/cm²), the nonlinear spectrum is completely positive. As the excitation intensity is increased, the low-energy part of the nonlinear PL due to each SQW becomes negative, and finally for intensities greater than 150 W/cm² the whole spectrum becomes negative. We attribute this to the population of an increasingly larger portion of the localized exciton states which give rise to the PL signal at low temperatures.

In Fig. 3(a) we present the NLPL signal from the 9 Å QW of sample A, as a function of the delay (solid line). The longest delay achievable was limited by the length of the translation stage (0.5 m). In Fig. 3(b) we present the PL decay curve (solid line) of the same spectral line measured at the same excitation intensity, using the APD. The incident photon energy and intensity in these measurements were 1.42 eV and 25 W/cm², respectively. These correspond to a carrier density of the order of 4×10^9 cm⁻². As can be seen in Fig. 3, both experimental techniques measure the same lifetime. We have verified this result for the series of SQWs in the two different samples. Moreover, the same results were obtained when the excitation energy was above the InP band gap, so that carriers were excited mainly in the barriers. The results were also found to be insensitive to the monitoring energy within one spectral line and to the excitation intensity within one or-

^{a)}Present address: Physics Department, Technion, Haifa 32000, Israel.

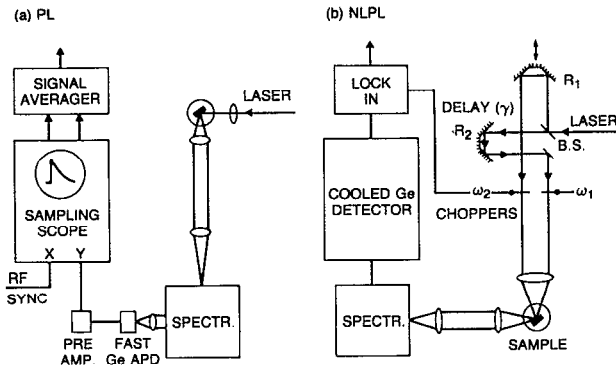


FIG. 1. Schematic diagram of the experimental setup. (a) PL decay times: The dispersed PL from the sample is tightly focused onto a fast Ge avalanche photodiode followed by a sampling oscilloscope and a signal averager. The temporal response is 300 ps. (b) Time dependence of the NLPL: The laser beam is split into two equal parts, each one is delayed with respect to the other and chopped at a different frequency. Both beams are focused on the sample, and the resulted emission is detected at the difference frequency by a lock-in amplifier.

der of magnitude. In particular the same decay behavior is observed regardless of the sign of the NLPL.

The low-temperature PL of semiconductor QWs is known to be excitonic in nature. For relatively low excitation intensities the PL is always due to recombination of excitons bound to shallow potential centers. These centers are either extrinsic, such as impurities, defects, and interface roughness, or intrinsic, such as the random potential caused by composition fluctuations in the alloy material. In

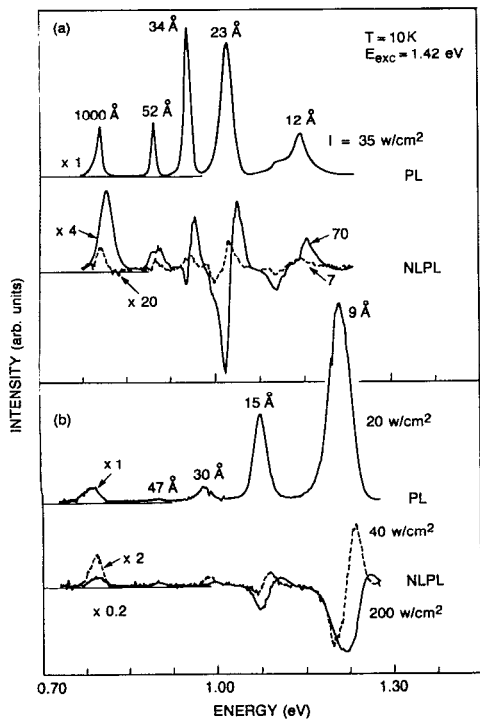


FIG. 2. Low-temperature PL (upper curves) and NLPL (lower curves) of the samples under study. (a) GSMBE-grown sample, (b) MOMBE-grown sample. The solid and dashed NLPL spectra were obtained with different excitation intensities.

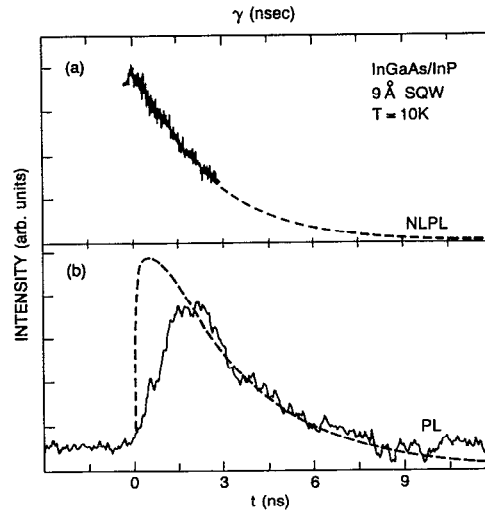


FIG. 3. (a) Measured NLPL autocorrelation signal (solid line) and the corresponding model calculation (dashed line). (b) Time-resolved PL (solid line) measured at the same conditions of (a), together with the calculated excitonic population $n_b(t)$ (dashed line).

InGaAs/InP heterostructures, the compositional fluctuations provide the most important contribution to these binding processes. This is usually evidenced by a pronounced Stokes shift, the inhomogeneous broadening of spectral lines¹² and the absence of a mobility edge along the excitonic luminescence band.¹³ The temporal evolution of the excitonic distribution function $F(E,t)$ can be described by the following rate equation, assuming that there is no correlation between the energy of the localized exciton and its position in space:

$$\begin{aligned} \frac{d}{dt}F(E,t) = & G\delta(E_l - E)\delta(t) - \frac{F(E,t)}{\tau_R} \\ & - \frac{F(E,t)}{n(E)} \int \frac{dE'}{\tau_{tr}(E,E')} [D(E') - F(E',t)] \\ & + \int \frac{dE'}{\tau_{tr}(E',E)} \frac{[D(E) - F(E,t)]}{n(E)} F(E',t). \end{aligned} \quad (1)$$

In Eq. (1), $D(E)$ is the excitonic density of states, $n(E) = \int_0^E D(E') dE'$ is the number of exciton states up to an energy E , τ_R is the radiative decay time of the excitonic population (assuming it is energy independent), $\tau_{tr}(E,E')$ is the time for excitons with an energy E to transfer to states of energy E' , and G is the generation rate of excitons by the laser pulse at the energy E_l and time $t = 0$.

In the absence of an *a priori* knowledge of the functions $D(E)$ and $\tau_{tr}(E,E')$, we have chosen to make some simplifying assumptions in order to solve Eq. (1). Under these physical assumptions the numerical solution of the model is much easier but yet it is capable of correctly predicting the experimental observations. We define a demarcation energy E_D such that excitons with energies higher than E_D can thermalize to states with energies lower than E_D ; excitons with energies lower than E_D are in terminal states,¹⁴ from which they can only recombine radiatively. Thus, we have reduced the problem to a two-level problem, where

TABLE I. Measured decay times of the single quantum wells.

Sample A: (HSMBE)		Sample B: (MOMBE)	
Well width (Å)	Decay time (ns)	Well width (Å)	Decay time (ns)
9 ± 2	3.0 ± 0.2	12 ± 3	4.1 ± 0.2
15 ± 3	2.5 ± 0.2	23 ± 3	3.6 ± 0.2
30 ± 3	2.1 ± 0.2	34 ± 4	4.0 ± 0.2
		52 ± 4	2.6 ± 0.2

we are concerned only with the temporal evolution of two excitonic populations: above $[n_a(t)]$ and below $[n_b(t)]$ the demarcation energy E_D . Mathematically expressed, we define

$$\frac{1}{\tau_{tr}(E, E')} = \begin{cases} (1/\tau_{ab}) & E > E_D; E' < E_D \\ 0 & \text{otherwise} \end{cases} \quad (2)$$

Now Eq. (1) is integrated with respect to E to yield two coupled rate equations:

$$\begin{aligned} \frac{d}{dt} n_a(t) &= G\delta(t) - \frac{1}{\tau_R} n_a(t) - \frac{1}{\tau_{ab}N_b} n_a(t)[N_b - n_b(t)] \\ &\times \frac{d}{dt} n_b(t) = -\frac{1}{\tau_R} n_b(t) + \frac{1}{\tau_{ab}N_b} n_a(t) \\ &\times [N_b - n_b(t)]. \end{aligned} \quad (3)$$

In Eq. (3) we have defined

$$N_b = n(E_D) = \int_0^{E_D} D(E) dE,$$

$$n_a(t) = \int_{E_D}^{\infty} F(E, t) dE,$$

$$n_b(t) = \int_0^{E_D} F(E, t) dE.$$

The linear PL resulting from a single laser pulse at $t = 0$ is given by $I_1 = \int_0^{\infty} n_b(t) dt$. The NLPL signal detected at the difference frequency $(\omega_1 - \omega_2)$ is calculated as¹⁰

$$I_{NLPL}(\gamma) = [I_2(\gamma) - 2I_1], \quad (4)$$

where $I_2(\gamma)$ is the PL resulting from both laser pulses being present at the sample at $t = 0$ and $t = \gamma$. That is, instead of $\delta(t)$ in Eq. (3), we have to substitute $(1/2)[\delta(t) + \delta(t - \gamma)]$.

There are three free parameters in the model: N_b (measured in units of G) τ_R , and τ_{ab} . The dashed line in Fig. 3(a) shows the calculated I_{NLPL} signal as a function of γ , and the dashed line in Fig. 3(b) corresponds to $n_b(t)$. Both curves were obtained using $\tau_R = 3$ ns, $\tau_{ab} = 50$ ps, and $G/N_b = 1.5$. As can be seen in Fig. 3, with these values the model describes very well both the temporal behavior of the PL and that of the NLPL. Moreover, we typically calculate the NLPL to be between 5% to 20% of the PL signal, in very good agreement with the experiment as can be seen in Fig. 2. The large difference between τ_R and τ_{ab} results in an almost exponential decay of the PL and the NLPL, with the same characteristic lifetime given by τ_R . The measured radiative lifetimes of all the QWs are listed in Table I. The other time constant τ_{ab} describes essentially

the time it takes the excitons to be formed and then to reach the states from which they can only recombine radiatively. The times for τ_{ab} that we extract from our fitting procedure are comparable with the formation time of excitons² and the spectral relaxation time¹³ measured previously. From the known generation rate one can estimate the excitonic saturation population density N_b . We obtain $(0.5 - 1) \times 10^{10} \text{ cm}^{-2}$, which is reasonable for a density of potential fluctuations estimated from the two-dimensional exciton area ($\sim \pi \times 150^2 \text{ \AA}^2$)

The NLPL signal results from the saturation of excitonic states; therefore, this signal is expected to be always negative. This is indeed the case for high enough excitation intensities, as can be seen in Fig. 2. We note that even though the two-level model is capable of predicting correctly the main features of the PL and the NLPL, it is too simple to explain all the observed details. The excitation intensity dependence of the NLPL spectral shape, the temporal decay insensitivity to changes in the excitation intensity, and the relatively long rise time of the PL (Fig. 3) cannot be accurately predicted by this model. It is obvious that in order to do that a more detailed modeling is required.

The PL decay times in Table I are relatively constant within each sample. This is expected for this range of QW widths.^{1,6} Clearly, the absolute values are sample dependent. The MOMBE sample shows decay times which are almost twice as long as those of the GSMBE sample, and about four times longer than previously reported results.⁶ The longer carrier lifetimes in the MOMBE-grown sample indicate the higher quality of that sample due to a reduced density of nonradiative recombination centers.

In summary, we have shown, both experimentally and theoretically, that decay times of the low-temperature PL from InGaAs/InP quantum wells can be directly measured using a PL autocorrelation technique.

¹J. Feldmann, G. Peter, E. O. Gobel, P. Dawson, K. Moore, C. Foxon, and R. J. Elliot, Phys. Rev. Lett. **59**, 2337 (1987).

²T. C. Damen, J. Shah, D. Y. Oberli, D. S. Chemla, J. E. Cunningham, and J. M. Kuo, J. Lumin. **45**, 181 (1990).

³J. Hegarty and M. D. Sturge, J. Opt. Soc. Am. **2**, 1143 (1985).

⁴J. Shah, IEEE J. Quantum Electron. **24**, 276 (1988).

⁵T. Takagahara, Phys. Rev. B **31**, 6552 (1985).

⁶U. Cebulla, G. Bacher, G. Mayer, A. Forchel, W. T. Tsang, and M. Razeghi, Superlattice Microstructure **5**, 227 (1989).

⁷M. G. W. Alexander, W. W. Rühle, R. Sauer, and W. T. Tsang, Appl. Phys. Lett. **55**, 885 (1989).

⁸D. Rosen, A. G. Doukas, Y. Budansky, A. Katz, and R. R. Alfano, Appl. Phys. Lett. **39**, 935 (1981).

⁹M. K. Jackson, M. B. Johnson, D. H. Chow, T. C. McGill, and C. W. Nieh, Appl. Phys. Lett. **54**, 552 (1989).

¹⁰M. B. Panish and H. Temkin, Annu. Rev. Mater. Sci. **19**, 209 (1989).

¹¹D. Ritter, M. B. Panish, R. A. Hamm, D. Gershoni, and I. Brener, Appl. Phys. Lett. **56**, 1448 (1990).

¹²D. Gershoni, H. Temkin, and M. B. Panish, Phys. Rev. B **38**, 7870 (1988).

¹³J. Hegarty, K. Tai, and W. T. Tsang, Phys. Rev. B **38**, 7843 (1988).

¹⁴J. A. Kash, Phys. Rev. B **29**, 7069 (1984).